BUTTERWORTH HEINEMANN

Polymer Vol. 36 No. 8, pp. 1655–1661, 1995

0032-3861/95/$10.00 + 0.00

Glass transition temperature regulation effect in a poly(vinyl alcohol)–water system

J. Rault*
Laboratoire de Physique des Solides, CNRS, 91405 Orsay Cedex, France

and R. Gref, Z. H. Ping, Q. T. Nguyen and J. Néel
Laboratoire de Chimie Physique Macromoléculaire, CNRS, URA-494, ENSIC, 1 rue Grandville, BP 451, 54001 Nancy Cedex, France
(Received 11 February 1994; revised 8 July 1994)

The temperature of crystallization and of melting of water in poly(vinyl alcohol) (PVA) membranes with various degrees of acetylation have been measured at different cooling and heating rates, and compared to the glass transition temperature (T_g) of the swollen materials. Above a certain critical concentration of water, c^*, when water begins to crystallize upon cooling, the T_g does not decrease according to the Fox equation, but remains constant. This phenomenon of regulation of the T_g and the origin of c^* are explained by the phenomenon of segregation of water in the amorphous phase during the process of crystallization. Finally, the effects of melting temperature depression and of broadening of the melting peak of ice in PVA–water systems, very similar to those observed in saccharose–water and alcohol–water mixtures, are explained by the phenomenon of dissolution, and not by the confinement effect.

(Keywords: membrane; poly(vinyl alcohol); glass transition)

INTRODUCTION

In hydrophilic polymers such as poly(vinyl alcohol) (PVA) and cellulose derivatives it has been postulated that absorbed water presents different states called bound and unbound[1–19]. Water in these systems is known to be affected by specific interaction (hydrogen bonding) with the polymer hydroxyl groups. D.s.c. studies have led to the conclusion that the amount of bound and unbound water is equal, respectively, to the amount of uncrystallizable and crystallizable water when the swollen polymer is cooled below 0°C. The aim of this paper is to show that in PVA the equivalence between bound water and uncrystallizable water is irrelevant and that the amount of uncrystallized water is governed by the phenomenon of regulation of the glass transition temperature (T_g) appearing during crystallization of water. Similar effects have been reported recently in sugar–water systems[20–22]. It is therefore important to compare, by d.s.c., the properties of swollen PVA with those of simple binary mixtures presenting the same type of interaction, and where confinement effects are absent.

EXPERIMENTAL

PVA 100%, 95% and 88% hydrolysed were supplied by Janssen chimica; the molecular weights are, respectively, 115 000, 95 000 and 96 000. N.m.r. analysis indicates that the chains have, respectively, $<0.2\%$, 2% and 12% acetyl residues.

PVA membranes, 100 mm thick, with crystallinity 25%, have been prepared by solvent evaporation of a solution of 7% PVA in water. The membranes were dried at 80°C for 4 h in an oven under vacuum and then swollen in water to equilibrium at 40°C. The water was then evaporated slowly to obtain homogeneous films having different water content c (mass concentration). The crystallinity of the dried membranes was determined by density measurements according to the method of Pritchard[23]. The crystallinity of the swollen membranes was deduced from the integrated intensity of the (1 1 0) reflection observed by X-ray and also from the amplitude of the 1142 cm^{-1} peak observed by i.r. spectroscopy[23–26]. The crystallization temperature (T_c) of water and the melting temperature (T_m) of ice in these membranes were measured by d.s.c. (Mettler) at various cooling rates (2.5, 5 and 10°C min^{-1}) and then extrapolated to zero cooling rate. The T_g was measured by dynamic mechanical thermal analysis[27,28] (d.m.t.a.; Polymer Laboratories) at 3 Hz in tension mode at a heating rate of 4°C min^{-1}. The materials were previously cooled to −140°C at a rate of 30°C min^{-1}. *Figures 1a* and *b* show typical d.s.c. and d.m.t.a. curves of swollen PVA (totally hydrolysed) membranes. The same types of curves were obtained for other PVA materials. One can distinguish two regimes in the swollen samples: a low concentration regime ($c < c^*$) where the water does not crystallize; and a high concentration regime ($c > c^*$) where crystallization is observed.

* To whom correspondence should be addressed

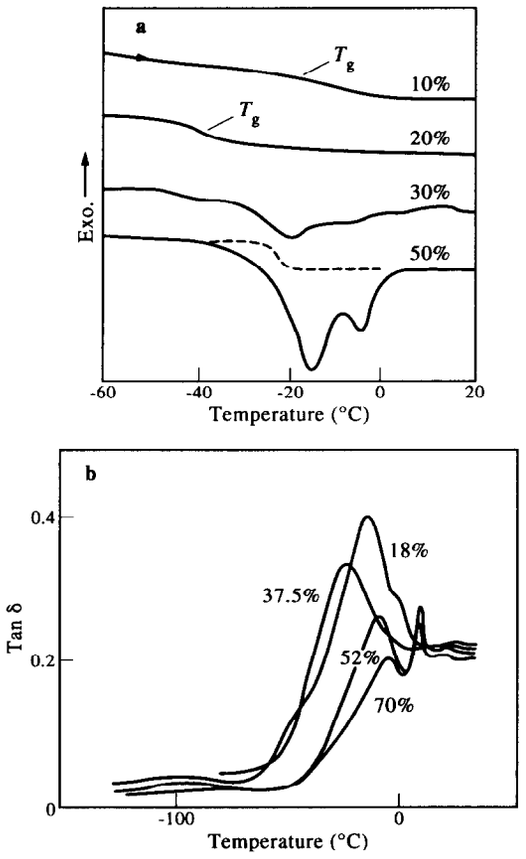

Figure 1 Typical d.s.c. (a) and d.m.t.a. (b) curves of swollen PVA membrane as a function of the water concentration (PVA is 100% hydrolysed). Heating rate: (a) 10°C min^{-1}; (b) 4°C min^{-1}

RESULTS

Glassy transition

D.s.c. measurements showed clearly that T_g varied with water concentration only in the range $0 < c < 30\%$. Above the critical concentration $c^* = 30\%$ this transition is not seen by d.s.c. and this suggests that the glass transition is hidden by the melting peak of ice. The jump in the heat capacity (ΔC_p) at the melting transition, represented by a dashed line in *Figure 1*, is due to the difference in the heat capacity of ice and water at the ice melting temperature and to the glassy transition of the amorphous PVA phase. The d.m.t.a. tan δ *versus* temperature plots at various heating rates showed the same results: the absence of a glass transition below -30°C for membranes in the second regime and a T_g decreasing with water concentration in the first regime. The small peak observed at -100°C is the well-known β secondary transition[28]. For concentrated membranes, the large d.m.t.a. peak observed between -30°C and 0°C is consistent with the glassy transition of the amorphous PVA phase and appears at the same temperature (or more exactly in the same temperature range) as the melting of ice. In the first domain ($c < c^*$) the amplitude of the glass transition peak tan δ increases from 0.1 for the dried sample to 0.4 for the swollen sample at c^* and then decreases slowly. The value of tan δ at the maximum is of the same order of magnitude as for hydrophilic copolymers polyamide 6 (PA 6)–poly(ethylene glycol) (PEG), and polyacrylamide (PAM). In all these systems T_g and tan δ vary in an opposite manner with the water content. In polyamide the increase of tan δ and the decrease of T_g with the water content has also been noted[29]. The T_g value at c^* is called T_g^*. In *Table 1* the T_g^*, c^* and tan* δ values are compared for different polymer–water systems.

Finally, it is to be noted that in dried PVA with some acetyl residues (up to 12%), the T_g is somewhat lowered. As plastication of PVA by acetyl residues is less important than by water, the variation of T_g with water concentration c (by weight) for all the PVA materials is shown in *Figures 2* and *3*. Below 40%, the experimental T_g curve follows the Fox–Flory[31,32] equation:

$$\frac{1}{T_g} = \frac{1-c}{T_g^P} + \frac{c}{T_g^w} \quad (1)$$

where T_g^P and T_g^w are the glass transition temperatures of pure PVA (80°C)[28] and pure water (-135°C according to Angell[33,34] and Razmussen and MacKenzie[35]). This relationship, verified by various polymer–solvent systems[36], indicates that water in PVA behaves like a typical classical plasticizer. In cellulose systems[7] and in PA 6 and PA 6.6[29] the variation of T_g with the concentration of water is greater than that predicted by the Fox law. The origin of this difference between PVA and PA and cellulose systems is not understood.

Melting transition of ice

As reported by many workers[1–18], d.s.c. curves for $c > c^*$ present two melting peaks, the temperatures T_m

Table 1 Critical parameters of polymer–water and sucrose–water systems[a]

	c^* (%)	n^*	T_g^* (°C)	Tan* δ
PVA				
100%	22	0.8	−30	0.4
88%	25	1.2	−30	0.4
PAM[b]	25	0.6	−25	
Sucrose[c]	18	0, 26	−32	

[a] n^* is the number of water molecules per monomer or sucrose molecule at the concentration c^* where ice formation begins. T_g^* and tan* δ are the glass temperature and the loss angle of the swollen membrane of concentration c^*

[b] Ref. 30

[c] Data from refs 20–22

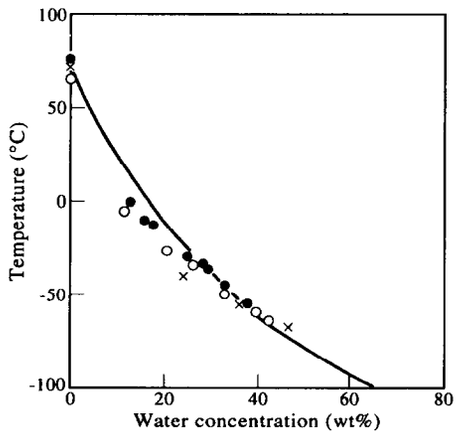

Figure 2 Glass transition temperature in swollen PVA membranes as a function of the water concentration, and as a function of the degree of acetylation of the polymer chains. The solid line represents the Fox–Flory relation. (●) PVA 100; (×) PVA 95; (○) PVA 88

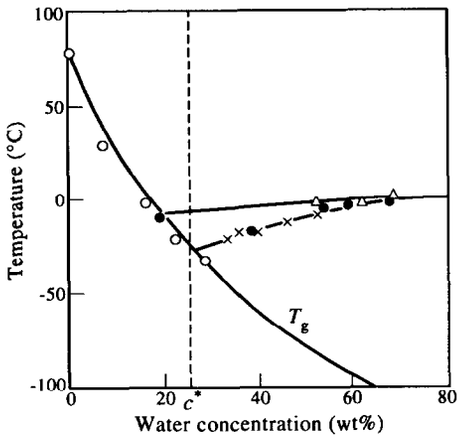

Figure 3 Glass transition melting and crystallization temperatures of swollen PVA membranes 100% hydrolysed. (○) T_g (d.s.c.); (●) T_g (d.m.t.a.); (△) T_{m1}; (×) T_{m2}

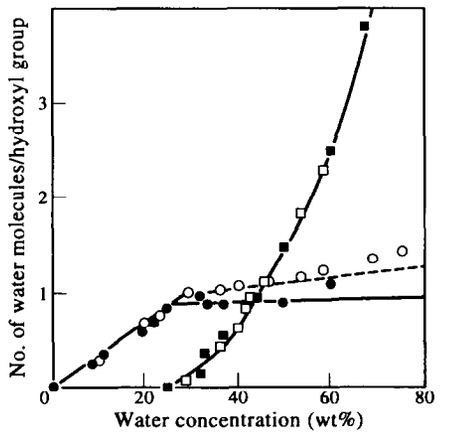

Figure 4 Number of crystallizable (squares) and uncrystallizable (circles) water molecules per hydroxyl group in PVA swollen membranes. (Open symbols) PVA 100; (solid symbols) PVA 88

and T'_m corresponding to the maximum of intensity and the widths of the peaks decrease with decreasing heating rate. The first peak T'_m, near 0°C, has been attributed to the free water present in pores created during the formation and/or swelling of the membrane. The exact origin of the T'_m peak in PVA and also in swollen cellulose acetate[17] and starch derivatives[19] is still unclear. The ratio $\Delta H/\Delta H'$ of the enthalpies corresponding to the two melting peaks depends weakly on the hydrolysis ratio and the cooling rate. The value of this ratio (~ 9) is greater than the value reported by others[5–16].

The T_m peak is located between -30°C and 0°C and depends on the concentration of water present. *Figure 3* shows the variation of T_g and T_m of the swollen membranes of 100% hydrolysed PVA. The same trends are observed for the membranes that are 98 and 88% hydrolysed. Two different regimes are clearly seen. The critical concentration c^*, above which crystallization of water is observed, is not dependent on the concentration of acetyl residues. *Figure 4* shows the number of crystallizable (n) and uncrystallizable (n^*) water molecules per hydroxyl group in the amorphous phase as a function of concentration. The number of crystallizable water molecules is deduced from the total enthalpy of melting ($\Delta H + \Delta H'$) over the whole range of temperature, and the change of crystallinity of the PVA chains as a function of c has been taken into account[26]. In our membranes it has been verified that the melting and crystallization enthalpies of water are equal. This is different to the result reported by Higuchi and Lijima[16]. It is assumed that the melting enthalpy of ice is temperature independent and equal to 334 J g^{-1}.

It is important to note that n^* and n for the PVA membranes with different acetyl rates show the same variations with c. A small difference is however noted for the value of c^* and n^*. This is related to the fact that all the PVA materials have the same T_g curve as shown in *Figure 2*. This suggests that c^* in these membranes is determined by the properties of crystallization of water and of the glassy state of the swollen polymer. In any binary liquid system (organic, inorganic, metallic) the crystallization of one component is possible only if the glass temperature of the liquid mixture is lower than the temperature of crystallization of that component.

Finally, the similarity of PVA–water and sucrose–water systems[20–22] should be emphasized. The T_gs of pure PVA and sucrose are, respectively, 80 and 70°C, the concentration c^* of unfrozen water in these swollen materials is, respectively, 22 and 18% and the T_g at this critical concentration is the same [$T_g(c^*) = -30$°C]. The similarity in c^* and $T_g(c^*)$ values is explained by the fact that the curves $T_g(c)$ and the liquidus $T_m(c)$ for the two systems are not very different.

DISCUSSION

T_g *regulation effect*

Figure 3 shows that when $c > c^*$ water crystallizes and the T_g of the material becomes equal to the T_m of ice. This phenomenon obviously must be quite general in a polymer–solvent system when the solvent crystallizes. The phenomenon of regulation of the T_g in these systems by crystallization of the solvent is described in *Figure 5*. In the swollen state, the T_g of the polymer–solvent system decreases with concentration according to the Fox–Flory

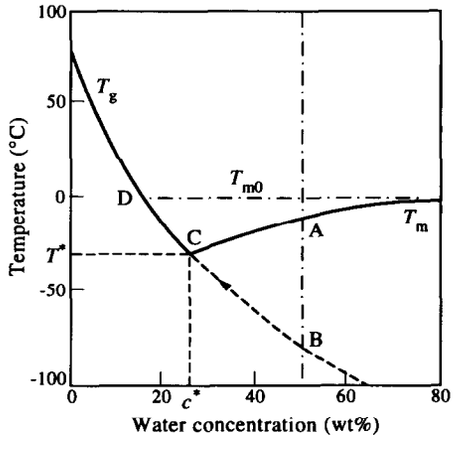

Figure 5 Phenomenon of T_g regulation by solvent crystallization in polymer systems. The intersection of the T_g curve with the T_m curve defines the critical concentration c^* below which the solvent cannot crystallize. T_m is assumed to vary with c according to the Raoult law. During crystallization the concentration of solvent in the amorphous phase decreases; therefore the T_g of the system increases and follows the dashed Fox–Flory curve. The process of crystallization stops when the figurative point reaches C. A similar effect occurs during the melting process

relation. Let us assume that the T_m of the solvent varies with concentration as shown in *Figure 5*. The exact form of the curve $T_m(c)$ has no importance here and will be explained in the next section. For simplicity it is assumed that there is no supercooling effect ($T_c = T_m$) and the concentration at the intersection (point C) of the two curves is called c^*. In the low concentration domain ($c < c^*$) the solvent does not crystallize for the simple reason that when lowering the temperature, the glass transition is passed through before the temperature of crystallization is reached. Hence, the system has been frozen before crystallization could occur. In the high concentration domain ($c > c^*$), during cooling, the material passes the T_m transition before reaching the glass transition. For example, a swollen polymer of concentration c_A is cooled from the liquid amorphous phase; when the temperature becomes equal to T_A, crystallization of the solvent in the liquid amorphous phase begins. After formation of some crystallites the concentration c of the remaining amorphous phase is $c = c_A - \Delta c$, the new equilibrium temperature of crystallization $T_m(c)$ is then lower than T_A, and crystallization is stopped and can continue only if the temperature of the system is lowered again. One must ask now if there is another phenomenon which stops at a certain temperature the crystallization of the solvent and therefore limits the total amount of solvent crystallites.

At the beginning of the process of crystallization the glass temperature of the amorphous phase (PVA plus solvent) of water concentration c_A is T_B (point B). As crystallization continues isothermally (at a very slow cooling rate) the solvent concentration in the amorphous phase decreases, and during this segregation the T_g of the material increases. (The figurative point of the liquid amorphous phase follows the dashed line representing the extrapolated Fox–Flory T_g curve.) The process of crystallization stops when the figurative point of the amorphous phase reaches point C, that is to say when the glass transition of the amorphous liquid phase becomes equal to the crystallization temperature of the solvent or, in other words, when at the temperature of crystallization the amorphous phase has been frozen. In this case the concentration of uncrystallizable solvent in the remaining amorphous phase is c^*. This effect explains why in PVA–water systems, the T_g does not follow the Fox–Flory equation when $c > c^*$, and why the T_g, observed by d.m.t.a., is nearly constant and equal to the T_m of ice. This effect also explains the c^* value, and therefore the number n^* of uncrystallizable water molecules per hydroxyl group which is not an integer: 0.8 and 1.2 for the 100% and 88% hydrolysed PVA (in the PAM–water system we have found that n^* is of the order of 0.6[30]). The PVA- and PAM–water membranes have the same characteristics (c^*, T_g^* and $\tan^* \delta$; *Table 1*) because these systems have similar $T_g(c)$ and liquidus $T_m(c)$ curves.

Origin of the variation of T_m *with* c

Most authors have explained qualitatively the melting temperature depression of ice in a polymer matrix in terms of confinement, that is to say by a capillary effect[1–17,36 43]. These effects in solid porous materials have been studied in detail[39–41]. According to Brun *et al.*[39] the pore size, r_p (in nm), is given by:

$$r_p = 0.57 + 65/\Delta T \tag{2}$$

where ΔT is the melting temperature depression of the ice crystallized in the pore. The thermoporometry method gives the pore size distribution in inorganic glass in accordance with other techniques.

The Brun *et al.* relation must be compared to the well known Thomson relation relating the T_m of a crystallite of finite size D[36,37]. The melting temperature of crystals growing in its supercooled liquid (no mixing entropy and no mixing enthalpy) is:

$$T_m = 273\left[1 - \left(\frac{2\sigma}{\Delta H}\right)\left(\frac{1}{D}\right)\right] = 273\left(1 - \frac{\beta}{D}\right) \tag{3}$$

which gives the melting temperature depression $\Delta T = 273\ \beta/D$. Here σ and ΔH are the surface energy and the melting enthalpy of an infinitely thick crystal per unit volume. It has been shown[37] that for all metals, $\beta = 2\sigma/\Delta H$ is constant and of the order of 1 nm, except for Li (0.4 nm) and Ge (3.3 nm). The same order of magnitude is observed for polymer monocrystals[36]. If one assumes that the β value of ice is of the same order of magnitude, the above two relations predict a melting depression temperature of 1 and 5°C for a crystal thickness of 50 nm and 10 nm.

The mean size of an ice crystal at −40°C in a PVA membrane ($c = 40\%$) has been measured by wide-angle X-ray scattering at the synchrotron source of LURE. The 100, 002 and 101 reflections of hexagonal ice give, according to the Debye and Scherer relation, a crystallite size of 50 nm[44,45]. One concludes that confinement alone cannot explain the high value of the melting temperature depression observed in PVA and PAM membranes (10–20°C).

Some authors[38–43] claim that the above thermoporometry relation also applies for solvent (water) in polymer, but they have not discussed the origin of this confinement of the water molecules in the polymer membrane (in the liquid state as opposed to inorganic membranes in the solid state). Finally, it should be recalled that Boonstra *et al.*[46] showed that the size of solvent crystallites in crosslinked rubber could not explain the important freezing point depression. These authors were the first, to our knowledge, to have suggested that 'the crystal size of the solvent may be limited not for mechanical reasons, but because at the boundary of the crystallites the solvent–polymer must be considered as a binary mixture with a well-defined temperature–composition diagram'.

In our polymer–solvent system as in binary liquid mixtures the endotherm peak observed by d.s.c. is not due to the melting process of the solvent, but rather to the dissolution of the solvent crystallites in a solution of polymer whose concentration varies during the process of dissolution. The variation of the ice melting temperature with concentration is given by the Flory–Huggins theory for polymer–water systems and by the Raoult law in binary mixtures of liquids. It is then important to compare the experimental results with the prediction of both theories.

Dissolution effect: Flory–Huggins approach

In the mean field approximation[32], the free energy of

mixing of polymer and solvent per site is:

$$F_s/kT=\frac{\varphi_P}{N}\log\frac{\varphi_P}{N}+\varphi_s\log\varphi_s+\chi\varphi_P\varphi_s \quad (4)$$

where $\varphi_P=1-\varphi_s$ is the fraction of sites occupied by monomers and χ is the interaction coefficient between monomer and solvent. For simplification one has to assume that the molar volumes of both species are equal. The first term, which represents the translational entropy of a chain of N monomers, disappears in gels and semicrystalline polymers. If the solvent crystallizes, the solvent T_m is a function of concentration. The equality of the chemical potential of the solvent in solution (μ_s^s) and in the crystalline state (μ_s^c) can be written as:

$$\mu_s^s=\varphi_P^2\frac{\partial}{\partial\varphi_P}\left(\frac{F_s}{\varphi_P}\right)=$$

$$\mu_s^c=\Delta H\left(\frac{T_m}{T_m^0}-1\right) \quad (5)$$

where T_m^0 is the melting temperature of the pure solvent, and ΔH the enthalpy of crystallization per solvent molecule.

At equilibrium, the T_m of solvent crystallites is then given by:

$$\frac{1}{T_m}-\frac{1}{T_m^0}=\frac{R}{\Delta H_m}[-\log(1-\varphi_P)-\varphi_P-\chi\varphi_P^2] \quad (6)$$

where ΔH_m is the enthalpy of crystallization per mole, and R is the gas constant. For a large concentration of solvent ($\varphi_P\ll 1$):

$$\frac{1}{T_m}-\frac{1}{T_m^0}=\frac{R}{\Delta H_m}\varphi_s^2(\tfrac{1}{2}-\chi) \quad (7)$$

Equation (6), reported by Orwoll[47], has not been applied to a polymer–solvent system to our knowledge. This expression implies that the mean field approximation is valid and that the chains have no translational entropy and no configurational entropy.

It is interesting to compare the Flory–Huggins prediction to the Raoult law valid for simple binary mixtures:

$$\frac{1}{T_m}-\frac{1}{T_m^0}=\frac{R}{\Delta H_m}\log a \quad (8)$$

where a is the activity which is reduced to the molar concentration of the species which crystallizes in the case of an ideal solution.

If one assumes that the polymer–water system is comparable to a simple binary mixture the above expression becomes:

$$\frac{1}{T_m}-\frac{1}{T_m^0}=\frac{R}{\Delta H_m}\log x \quad (9)$$

where x is the molar fraction of monomers of molecular weight = 42.

To compare the experimental data with the theoretical prediction of equations (6)–(8), T_m values of ice in PVA have been measured as a function of the heating rate and concentration. All the samples (*Figure 6a*) show a linear relation between T_m and the heating rate V in the case of PVA membrane 100% hydrolysed having a concentration $c=33\%$ and 43% water. Similar linear

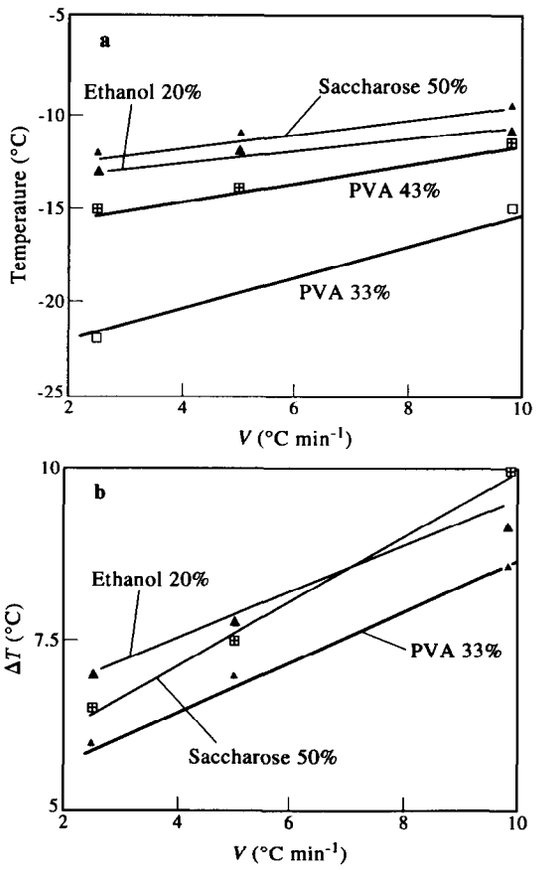

Figure 6 (a) Dependence of the melting temperature T_m of ice crystallites in PVA with 33 and 43 wt% water as a function of the d.s.c. heating rate V. The T_m of ice in water–saccharose solutions ($c=50\%$) and in water–ethanol solutions ($c=20\%$) are also shown. (b) Width of the ice melting peaks $\Delta T(1/2)$ observed by d.s.c. as a function of the heating rate V: water–saccharose system ($c=50\%$), ethanol–water system ($c=20\%$) and PVA–water system ($c=33\%$)

plots were obtained for different concentrations and for the different PVAs. One recalls here that T_m corresponds to the maximum of the endothermic peak (and not to the onset of the peak as it is known for melting transitions). From *Figure 6* it can be concluded that the variation of the ice melting depression with the heating rate in the PVA system and in simple binary mixtures of equivalent molar concentration are of the same order of magnitude.

Figure 7a shows the variation of the ice melting temperature with the concentration of water in PVA (curves A and B) and in ethanol (curve D). Raoult plots (curve C) and the experimental curve B extrapolated at zero heating rate show the same trend and a finite slope at high concentration of water ($c\sim 1$).

In *Figure 7b* a comparison is made of the predictions of the Flory–Huggins approach and that of the Raoult law. The Flory–Huggins plots have been drawn for three different values of the interaction parameter χ. The experimental value of χ for the PVA–water system, measured by Sakurada *et al.*[1] and Hamada *et al.*[18,48], respectively, by vapour pressure measurement and by the melting point depression of the polymer, is $\chi=0.49$. It must be stressed that these measurements were done in semi-dilute solution ($1>c>0.85$), whereas for our experimental data $0.7<c<0.25$, and that the properties measured by these authors probably depend on the

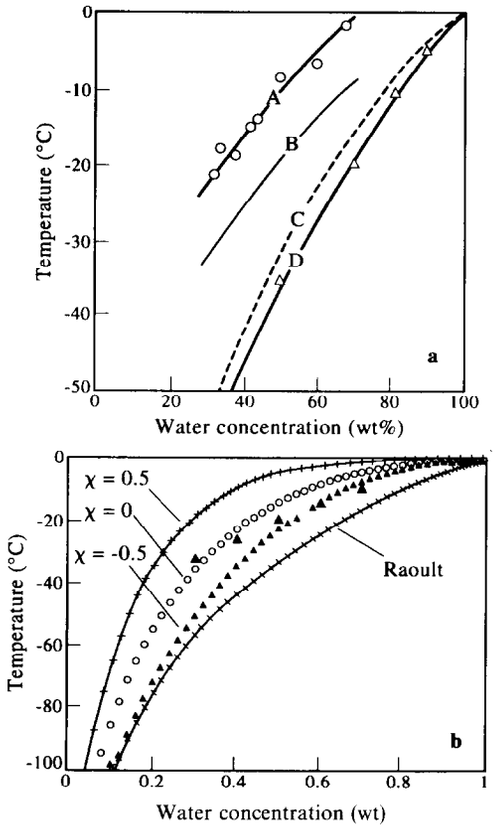

Figure 7 (a) Melting temperature curves (A–C) of ice crystallites in PVA 100% hydrolysed ($c=33\%$) and in ethanol solution (D) as a function of concentration: (A) experimental data, d.s.c. at 10°C min^{-1}; (B) extrapolated d.s.c. values at a very slow cooling rate, see *Figure 6a*; (C) theoretical prediction from the Raoult law; (D) water–ethanol solution ($c=20\%$), d.s.c. at 5°C min^{-1}. (b) Melting temperatures of ice in polymer–water systems predicted by the Flory–Huggins relation for three values of the interaction parameter χ. (▲) Experimental data extrapolated for heating rate $V=0$ (deduced from *Figure 6a*). The prediction of the Raoult law is also reported

crystallinity of the polymer and therefore on the preparation of the membrane. It should be emphasized that low molecular weight PVA is completely dissolved by water[20]; water is a good solvent and not a theta solvent.

From *Figure 7b* it can be concluded that the experimental curve (extrapolated to zero cooling rate) lies between the theoretical Flory–Huggins curve ($\chi \sim -0.5$) and the Raoult curve (ideal solution). The discrepancy between the Flory–Huggins and experimental curves could be due to a variation of χ with concentration but no variation has been reported for a dilute solution. We believe that this discrepancy arises for a more fundamental reason; the configurational entropy is not taken into account by the Flory theory, and the mixing entropy is overestimated by the Raoult law.

Origin of the broadening of the melting peak

The greater width of the ice melting peak in PVA and other polymer–water systems has been noted by many authors[1–16,41–44] and interpreted as being due to the distribution of size of the crystals of ice, which in turn would be due to the distribution of pores. In all the reported studies, the d.s.c. heating rates were 10 or 20°C min^{-1}. The variation of the width of the melting peak T_m with the heating rate has not been studied to our knowledge.

In fact, this effect is also observed in binary simple mixtures. In *Figure 6b* a comparison is made of the width $\Delta T(1/2)$ at half height of the melting peak of ice in PVA, saccharose and ethanol solutions of similar molar concentration ($x=10\%$) as a function of the heating rate. The $\Delta T(1/2)$ value decreases with the heating rate V for the different types of materials but is not extrapolated to 0°C as it is observed for pure water. The extrapolated values at $V=0$ are 5, 6.2 and 5.3°C for, respectively, saccharose, ethanol and PVA systems of similar molar concentration (respectively, of mass concentration 50, 20 and 33%). This indicates that the origin of the broadening is not due to kinetic effects. The broadening of the ice melting peak is obviously related to the fact that the temperature of ice melting is a function of concentration; the T_m melting peak is in fact a dissolution peak as shown in *Figure 5*.

A PVA–water system with a water concentration c_A higher than the critical concentration c^* has been crystallized and its melting transition studied during a d.s.c. scan. For sake of clarity it is assumed that the water crystallization occurred at T_A (no supercooling), and after crystallization, as explained above, the remaining concentration of water in the amorphous phase is c^* and not c_A. When this material is heated up melting begins at T^* (point C) and the concentration of water in the amorphous phase increases during melting. Melting can carry on only if the temperature is increased. During a d.s.c. scan, the process of melting is continuous (even at a very low heating rate) and stops (point A) when the concentration of water in the amorphous phase becomes equal to C_A. *Figure 5* shows that the width of the d.s.c. peak is equal to $T_A - T^*$ and therefore increases with the gap concentration $c-c^*$, even if the heating rate is infinitely small as observed experimentally.

The comparison between PVA–water systems and a binary simple mixture shows that the broadening of the ice melting (and crystallization) peaks is not due to confinement of ice crystals but to dissolution effects.

CONCLUSIONS

Crystallization of water or any solvent in a binary system involves segregation and therefore a decrease in the concentration of these species in the remaining liquid phase. The important consequence is that the characteristics (in particular the T_g) of the liquid phase change during the crystallization process. The phenomenon of regulation of the T_g of the polymer–water system by crystallization of the solvent explains the critical concentration c^* at which water begins to crystallize; c^* is given by the intersection of the melting temperature curve $T_m(c)$ with the glass transition temperature curve $T_g(c)$. Below c^*, water cannot crystallize, not because water is bound, but because the glassy state of the polymer–water system is reached before the temperature of water crystallization. The concentration c^* can be modified by the presence of salts and organic compounds which change the temperature of crystallization of water and the T_g of the ternary system as observed by Zhang *et al.*[5]. In PVA–PVP blends T_g increases with the concentration of PVP. In the swollen blend the $T_g(c)$ curve is then shifted towards high

temperatures; the intersection of the T_g curve with the ice solidus $T_m(c)$ is also shifted. In that case the critical concentration c^* and temperature T_g^* increase continuously with the concentration of PVP in the blend[50].

Finally, it has been shown that the melting temperature curve $T_m(c)$ of ice above c^* lies between the Raoult theoretical curve giving the dissolution temperature of crystallizable species in a binary system and the theoretical curve deduced from the Flory–Huggins theory (good solvent). The broadening of the ice melting peak observed by d.s.c. even at low heating rate is explained by the progressive increase in concentration of water in the amorphous phase during the melting process. These two effects are qualitatively and quantitatively similar to those observed in simple binary systems like water–ethanol and water–saccharose. The described phenomenon of regulation should apply to any homogeneous organic, inorganic or metallic system. We must note that the supercooling effect and the presence of heterogeneities in polymer–solvent systems (pores, fluctuation of chains and crosslinks, segregation[50]) would complicate our analysis.

REFERENCES

1 Sakurada, I., Nakajima, A. and Fujiwara, H. *J. Polym. Sci.* 1959, **35**, 497
2 Kenney, J. F. and Willcockson, G. W. *J. Polym. Sci.* 1966, **A4**, 679
3 Takizawa, A., Negishi, T. and Ishikawa, K. *J. Polym. Sci.* 1968, **A6**, 475
4 Peppas, N. A. and Merril, E. W. *J. Appl. Polym. Sci.* 1976, **20**, 1457
5 Zhang, W. Z., Satoh, M. and Komiyama, J. *J. Membr. Sci.* 1989, **42**, 303
6 Shibukawa, M., Ohta, N. and Onda, N. *Bull. Chem. Soc. Jpn* 1990, **63**, 3490
7 Kolov, Yu. M., Kynin, A. T., Nikolaev, A. F. and Grebennikov, S. F. *Zhurnal Prikladnoi Khimii* 1989, **62**, 1673
8 Hatakeyama, T., Hirose, S. and Hatakeyama, H. *Makromol. Chem.* 1989, **184**, 1265
9 Hatakayama, T. and Yamauchi, A. *Eur. Polym. J.* 1984, **20**, 61
10 Hatakeyama, T., Ikeda, Y. and Hatakeyama, H. *Makromol. Chem.* 1987, **188**, 1875
11 Nishioka, N., Yamaguki, A. H. and Kosai, K. *Jpn Appl. Polym. Sci.* 1990, **40**, 2007
12 Uragami, T., Sugitani, Y. and Sugihara, M. *Polymer* 1982, **23**, 192
13 Gurghoff, H. G. and Pusch, W. *J. Appl. Polym. Sci.* 1981, **26**, 2625
14 Carles, J. E. and Scallan, A. M. *J. Appl. Polym. Sci.* 1973, **17**, 1855
15 Fushimi, H. and Lijima, T. *Polymer* 1991, **32**, 241
16 Higuchi, A. and Lijima, T. *Polymer* 1985, **26**, 1208
17 Taniguchi, Y. and Horigome, S. *J. Appl. Polym. Sci.* 1975, **19**, 2743
18 Hamada, F., Nakajima, A. and Fujimara, A. *Kobunshi Kagaku* 1966, **23**, 395
19 Roadehed, C. and Ranby, B. *J. Appl. Polym. Sci.* 1986, **32**, 3309
20 Frank, F. in 'Properties of Water in Foods' (Eds D. Simatos and J. L. Multon), Martinus Nijhoff, Dordrecht, 1985
21 Hatley, R. H., Van den Berg, C. and Franks, F. *Cryo Lett.* 1991, **12**, 113
22 Simatos, D. and Blond, G. in 'The Glassy State of Foods' (Eds J. M. Blanchard and P. Lillford), Nottingham University Press, Nottingham, 1993
23 Pritchard, J. G. 'Polyvinyl alcohol: Basic Properties and Uses', Gordon and Breach, New York, 1970
24 Peppas, N. A. *Makromol. Chem.* 1977, **178**, 595
25 Peppas, N. A. and Merill, E. W. *J. Polym. Sci. Polym. Chem. Edn* 1976, **14**, 441
26 Greff, R. *PhD Thesis* University of Nancy, 1991
27 Takayanagi, M. *Mem. Fac. Eng. Kyushu Univ.* 1963, **23**, 1
28 McCrum, N., Read, B. and Williams, G. (Eds) 'Anelastic and Dielectric Effects in Polymeric Solids', Wiley, New York, 1967
29 LeHuy, M. and Rault, J. *Polymer* 1993, **35**, 136
30 Rault, J., Ping, Z. and Nguyen, T. *J. Non Cryst. Mater.* 1994, **172–174**, 733
31 Fox, T. G. and Flory, P. J. *J. Polym. Sci.* 1954, **14**, 315
32 Flory, P. J. 'Polymer Chemistry', Cornell University Press, Ithaca, 1971
33 Angell, C. A. in 'Water: a Comprehensive Treatise' (Ed. F. Franks), Vol. 7, Plenum Press, New York, 1982, pp. 11–81
34 Angell, T. *J. Chim. Phys.* 1980, **84**, 268
35 Rasmussen, D. H. and MacKenzie, A. P. *J. Phys. Chem.* 1971, **75**, 967
36 Elias, H. G. 'Macromolecules', Plenum Press, New York, 1977
37 Wautelet, M. *J. Appl. Phys.* 1991, **24**, 343
38 Nagura, M., Nagura, M. and Ishikawa, H. *Polymer* 1984, **25**, 313
39 Brun, M., Lallemand, A., Quinson, J.-F. and Eyraud, C. *Thermochim. Acta* 1977, **21**, 59
40 Klafter, J. and Drake, J. (Eds) 'Molecular Dynamics in Restricted Geometries', Wiley, New York, 1989
41 Handa, Y. P., Zakrzewski, M. and Fairbridge, C. *J. Phys. Chem.* 1982, **86**, 998
42 Cuperus, F. P., Bargeman, D. and Smolders, C. A. *J. Membr. Sci.* 1992, **66**, 45
43 Desbriere, J., Rinaudo, M., Brun, M. and Quinson, J. F. *J. Chim. Phys.* 1981, **78**, 187
44 Dowell, L. G. and Rinfret, A. P. *Nature* 1960, **188**, 1144
45 Guinier, A. 'Theory et Technique de la Radiocristallographie', Dunod, Paris, 1956
46 Boonstra, B. B., Heckman, F. A. and Taylor, G. L. *J. Appl. Polym. Sci.* 1968, **12**, 223
47 Orwoll, R. A. *Rubber Chem. Technol.* 1982, **50**, 451
48 Hamada, F. and Nakajima, A. *Kobunshi Kagaku* 1966, **23**, 395
49 Ping, Z. *PhD Thesis* Nancy, 1994
50 Stocks, W. and Berghmans, H. *J. Polym. Sci., Polym. Phys. Edn* 1991, **29**, 609